Theoretical Study of Photochemical Mechanisms of C_3O Formation

Scott Ekern and Martin Vala*

Department of Chemistry and The Center for Chemical Physics, University of Florida, Gainesville, Florida 32611

Received: December 3, 1996; In Final Form: March 10, 1997[⊗]

Photolysis of the $C_3{\cdot}H_2O$ complex in an argon matrix with $\lambda \geq 400$ nm leads to the formation of propynal and tricarbon oxide. One pathway to the formation of propynal has been shown experimentally and theoretically to involve the intermediate hydroxypropadienylidene (HPD). This intracomplex mechanism involves the photoinitiated insertion of C_3 into an OH bond of water followed by migration of H atoms along the CCCO backbone to form the end product, propynal. The mechanism by which tricarbon oxide, C_3O, is formed is examined in this investigation. To probe this pathway, the H_2C_3O potential surface, including H atom loss and later attachment, has been calculated at the MP2/6-31G* level of theory. It is shown that two photoconversion pathways exist. One leads to HPD (and thence to propynal), while the other involves H atom loss to a HC_3O intermediate, which then either loses another hydrogen atom to form C_3O or captures a hydrogen atom to produce propynal. In addition, bimolecular mechanisms involving C atoms, C_2, and C_nO molecules are explored to determine whether they might also yield C_3O. Finally, the possible importance of all these reactions in the production of C_3O and propynal in the mantles of interstellar dust grains is discussed.

I. Introduction

The complex between the small carbon cluster C_3 and water was first identified in a rare gas matrix by Ortman, Hauge, Margrave, and Kafafi in 1990.[1] Photolysis of the $C_3{\cdot}H_2O$ complex was shown to yield C_3O and propynal. The photoproducts were further demonstrated to be wavelength-dependent. Irradiation spanning the first electronic transition of the $C_3{\cdot}H_2O$ complex at 405.4 nm resulted in formation of C_3O, propynal, and an intermediate now known[2] to be 3-hydroxypropadienylidene (HPD). Irradiation with wavelengths between 280 $\leq \lambda \leq$ 320 nm led to the production of propynal, which after further photolysis converts to CO and acetylene. The experimental scheme is given in Figure 1.

Recently, *ab initio* calculations have been used to characterize the potential energy surfaces leading from the $C_3{\cdot}H_2O$ complex via HPD to propynal and finally to CO and acetylene.[3] The model involves initial insertion of the C_3 molecule into the OH bond of water followed by a series of hydrogen migrations along the CCCO backbone. Finally, dissociation of two C_3H_2O isomers leads to CO and acetylene. While this mechanism describes the experimental observations quite well, several questions remain. First, despite adequately describing how propynal forms via the HPD intermediate during the higher energy photolysis step, the mechanism of propynal formation in the lower energy photolysis step was not examined. Secondly, the mechanism of C_3O production remains undetermined. Does it also arise from the $C_3{\cdot}H_2O$ complex or by some other mechanism? Thirdly, the rationale behind the formation of C_3O in the first photolysis step, and not in the second, higher energy step, was not pursued. In this paper we present a calculational study of the C_3H_2O potential surface that characterizes the lower energy photolysis of $C_3{\cdot}H_2O$ to propynal and C_3O. The paper is laid out as follows. The theoretical procedures used are outlined in section II. In section IIIA, a mechanism for the photoconversion of the $C_3{\cdot}H_2O$ complex to both propynal and C_3O is proposed, and then, in section IIIB, several possible bimolecular mechanisms leading to the formation of C_3O are examined. Finally, in section IV, conclusions are drawn.

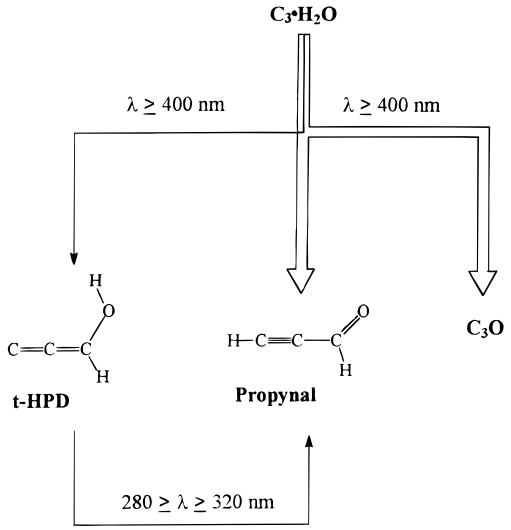

Figure 1. Schematic of possible multiple pathways from $C_3{\cdot}H_2O$ complex to photoproducts.

II. Theoretical Section

All calculations were carried out at the MP2/6-31G* level using the GAUSSIAN 94 program package.[4] The inclusion of electron correlation has been shown to be extremely important in obtaining correct geometries[5] and can have a profound effect on the quantitative aspects and even the content of potential energy surfaces.[3] Unless otherwise stated, all minima and transition states were optimized in their ground electronic states constrained to the symmetries given in Tables 1 and 2. Optimized structures of all minima and transition states are shown in Figures 2 and 3, respectively. The calculated surface represents the minimum energies necessary to promote reaction. Vibrational frequencies were calculated to determine the nature of the stationary point and to provide the thermochemical data necessary for corrections to the reaction energies. Internal reaction coordinate (IRC) calculations were performed to determine which minima connect with which particular transition states. The energy levels shown in Figure 4 represent points along the H_2C_3O potential surface. Those points that have no

[⊗] Abstract published in *Advance ACS Abstracts,* April 15, 1997.

S1089-5639(96)03960-6 CCC: $14.00

TABLE 1: Total Energies (hartrees), Zero-Point-Corrected Relative Energies (kcal/mol), Spin Squared Eigenvalues, and Zero-Point Energies (kcal/mol) of Minima Found at the MP2/6-31G* Level of Theory

molecule	sym	total energy*	relative energy	$\langle S^2 \rangle$	ZPE
A	C_s	−189.895 21	0.0	0.0	19.9
B	C_s	−189.997 78	−60.3	0.0	24.2
C	C_s	−189.988 86	−54.8	0.0	24.1
D	C_s	−189.997 71	−61.3	0.0	23.1
E	C_s	−190.086 63	−117.1	0.0	23.1
F	C_s	−189.374 38	13.3[a]	1.167	18.9
G	C_s	−189.343 49	30.9[a]	0.922	17.1
C(^{3}P)		−37.733 83		2.005	
C_2 ($^1\Sigma_g^+$)	$D_{\infty h}$	−75.696 17		0.0	2.7
C_2 ($^3\Pi$)	$D_{\infty h}$	−75.688 20		2.005	2.7
CO ($^1\Sigma^+$)	$C_{\infty v}$	−113.021 21		0.0	3.0
C_2O ($^3\Sigma^-$)	$C_{\infty v}$	−150.834 92		2.059	5.6
C_3O ($^1\Sigma^+$)	$C_{\infty v}$	−188.860 03		0.0	9.7
C_3O ($^3\Sigma^-$)	$C_{\infty v}$	−188.740 66		2.521	10.2
C_4O_2 ($^3\Sigma_g^-$)	$D_{\infty h}$	−301.896 13		2.151	15.8
H		−0.498 23		0.750	
H_2		−1.144 14		0.0	6.5

[a] Relative energy composed of stationary point and hydrogen atom total energies with zero-point correction.

TABLE 2: Total Energies (hartrees), Zero-Point-Corrected Relative Energies (kcal/mol), Spin Squared Eigenvalues, and Zero-Point Energies (kcal/mol) of Minima Found at the MP2/6-31G* Level of Theory

transition state	sym	total energy*	relative energy	$\langle S^2 \rangle$	ZPE
TS1	C_1	−189.848 43	27.9	0.0	18.4
TS2	C_1	−189.808 72	51.5	0.0	16.9
TS3	C_s	−189.327 87	35.0[a]	0.897	11.1
TS4	C_s	−189.304 59	49.5[a]	1.005	11.1
TS5	C_s	−189.796 85	58.2	0.0	16.2
TS6	C_s	−189.807 89	51.1	0.0	16.0
TS7	C_s	−189.834 44	36.1	0.0	17.8
TS8	C_s	−189.856 73	21.5	0.0	17.2
TS9	C_1	−189.969 86	−44.1	0.0	22.6
TS10	C_s	−188.709 73		2.040	10.3

[a] Relative energy composed of stationary point and hydrogen atom total energies with zero-point correction.

or only one hydrogen have the MP2/6-31G* H or H_2 energy added to them (at the infinite separation limit), to ensure that the H_2C_3O total energy is maintained. Before presentation of the results, a caveat is needed. Because the goal of this work has been the determination of the most probable pathway(s) to the formation of C_3O, via a calculation of the appropriate potential surface(s), a balance was sought between computational accuracy and computational speed. The choice of the MP2 approach with 6-31G* basis functions was felt to constitute a reasonable compromise. An MP2/6-31G* calculation can be expected to yield a qualitatively reliable potential surface, although higher level calculations will be necessary to obtain more accurate intermediate and transition state energies.

III. Results

For the surface modeled to be correct for the present system, it must lead ultimately to the formation of C_3O and propynal. We have shown previously that the precursor to propynal is the $C_3{\cdot}H_2O$ complex. The precursor(s) to C_3O may be the $C_3{\cdot}H_2O$ complex or one of several other precursors. One possible route to C_3O formation, which involves the $C_3{\cdot}H_2O$ complex, is

$$C_3{\cdot}H_2O + h\nu \rightarrow C_3O + 2H \text{ or } H_2 \qquad (1)$$

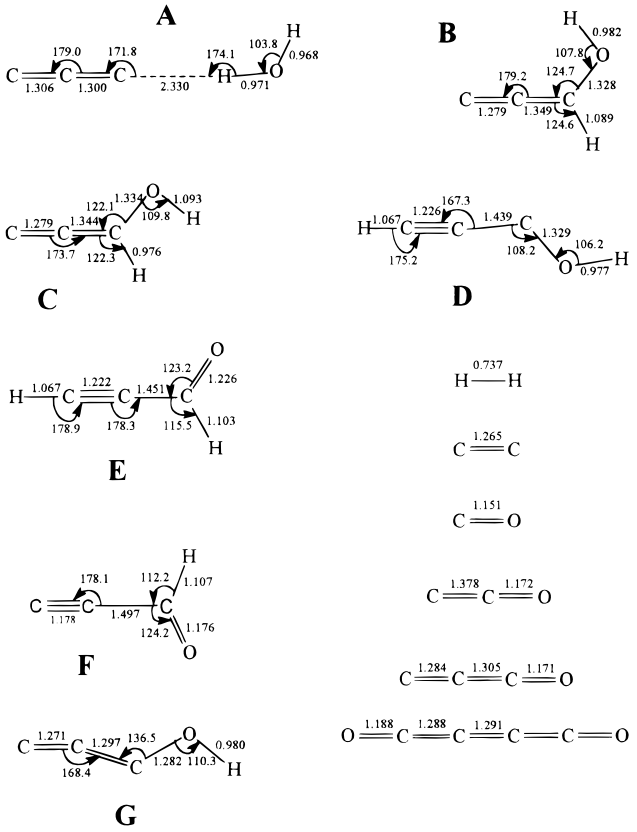

Figure 2. Optimized structures of all minima found at the MP2/6-31G* level of theory. Bond lengths are in angstroms, angles in degrees.

In the following section (IIIA), this mechanism is fully explored. Since carbon atoms C_2 and C_3 and water are all known to be present and abundant in the matrix after deposition, they must be considered as possible precursors to C_3O. In the next section (IIIB), several bimolecular reactions that may lead to C_3O formation are considered.

A. The C_3H_2O Potential Surface. We recently showed how a two-step photolysis involving a series of hydrogen migrations could produce propynal from the $C_3{\cdot}H_2O$ complex. However, a competing mechanism (cf. Figure 1) exists and may produce propynal during the first photolysis step (with $\lambda \geq 400$ nm). This process begins with the $C_3{\cdot}H_2O$ complex since no propynal, or any other product, is observed in the matrix prior to excitation of the 405 nm C_3 electronic transition. This observation leads to the presumption that there is another route for the production of propynal and C_3O. This alternate mechanism, unlike that in the previous paper, involves photolytic detachment of hydrogen, with later recombination. For such a mechanism to be operable, hydrogen atoms must be capable of diffusion through the matrix. There is strong evidence that this is possible. It has been shown that H atoms can migrate through matrices of H_2O,[6−8] CO,[9] and N_2.[10] After encountering other open shell species, H atoms can combine to form basic organic molecules like NH_3,[10] HCO, formaldehyde, and methanol.[9] Obviously, such a mechanism that incorporates H atom migration is required here since hydrogen is contained in the suspected precursor to C_3O, the $C_3{\cdot}H_2O$ complex.

Energetic photons, up to 71.5 kcal/mol (400 nm), are available during photolysis. This value places an upper limit on the step size (i.e., the energy difference) between points on the surface. The $C_3{\cdot}H_2O$ complex (**A**) has two outlet paths through transition states 1 and 2 (TS1 and TS2). We examine each of these in turn below.

From **A**, the HPD isomers **B** and **C** may be formed via transition state TS1. Although only a small barrier (TS9) exists

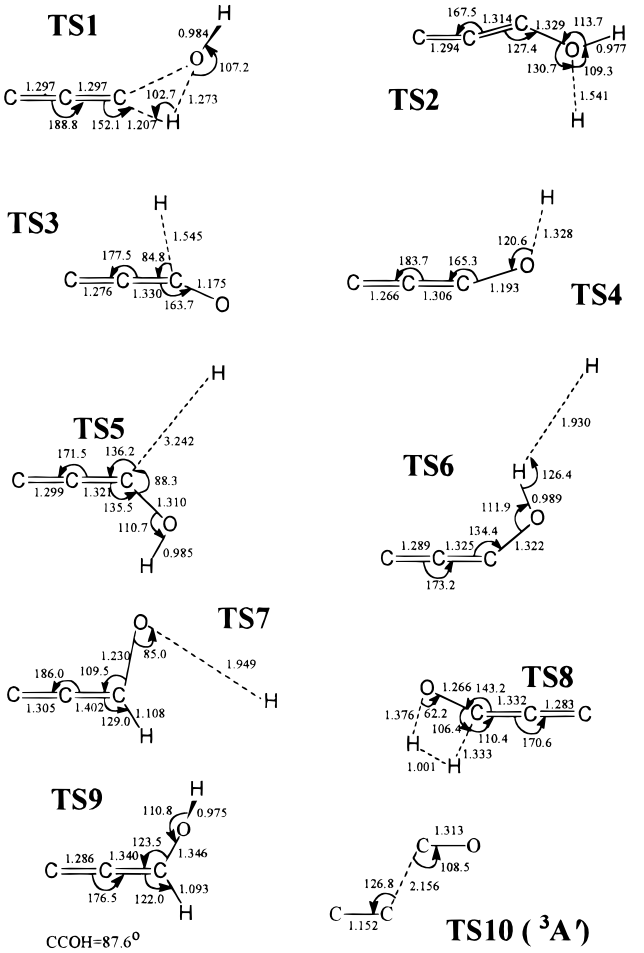

Figure 3. Optimized structures of all transition states found at the MP2/6-31G* level of theory. Bond lengths are in angstroms, angles in degrees.

between the HPD isomers, only **C** is seen during photolysis. The barrier for HPD conversion to propynal (**E**) in the previously studied hydrogen migration scheme is 87.0 kcal/mol,[3] making that particular path unavailable here. The only other route to propynal from HPD is via hydrogen atom dissociation and recombination. The most direct way this can be accomplished is through hydrogen loss from the oxygen, resulting in molecule **F**, followed by recombination at the terminal carbon. This is calculated to be a very exothermic reaction (130.4 kcal/mol). The step from **C** to **F** is predicted to require only 68.1 kcal/mol, but if there is a transition state more than 3 kcal/mol above **F**, this path will not be energetically accessible. Figure 4 shows that the transition state (TS7) from **C** to **F** lies almost 91 kcal/mol above **C**. However, this transition state does not represent the actual transition state. The real transition state is formed by the crossing of the singlet and triplet dissociation/recombination surfaces (Figure 5). In this calculation the O−H bond distance was increased stepwise by 0.2 Å, starting near the optimized cis-HPD O−H bond distance. At each point the remainder of the complex was allowed to relax, constrained only to C_s symmetry. As Figure 5 shows, there are two intersections between the singlet and triplet surfaces, but the limiting barrier here is at an O−H distance of ca. 1.82 Å. The intersection barrier of approximately 85 kcal/mol is only marginally smaller than the singlet surface barrier at TS7. Nevertheless, both barriers require more energy than is experimentally available, leading us to conclude that the process **C** (or **B)** to **F** (via TS7) does not occur during low-energy photolysis.

The ground state structure of **F** indicates that the unpaired electron resides primarily on the terminal carbon. Because of this, reaction between a H atom and **F** will more than likely lead to propynal formation in an extremely exothermic reaction (130.4 kcal/mol). Once **F** is formed, reaction with H atom at the terminal carbon will yield propynal. As shown in Figure 5, the reaction from **F** to **E** has a small barrier which is formed by the crossing of the singlet and triplet reaction surfaces. Dissociation along the triplet surface approaches the total energy of molecule **F** and the H atom at infinite separation, 130.4 kcal/mol above propynal and ca. 12 kcal/mol below the singlet−triplet intersection. A similar type of path is found for H loss from linear HC_3H.[10] While this barrier is a fraction of the reaction enthalpies or photolysis energies considered in this surface, it is more than adequate to keep propynal from being formed in the gas phase. In the absence of a photon or energetic reactants, such small barriers as this could actually *prevent* hydrogenation of gas-phase unsaturated species.

In addition, C_3O could form from HPD as well. There are only two possible reaction pathways. The first is **C** → TS8 → $C_3O + H_2$. The step from **C** to TS8 is calculated to require 76.3 kcal/mol. This is 5.2 kcal/mol more than the upper energy limit, and even considering the calculation error intrinsic in this level of theory, this route is probably not possible. The other path again involves hydrogen loss from **B** or **C** → **F** → TS3 → $C_3O + 2H$. Once **F** is formed there is just a 21.7 kcal/mol barrier to H loss and C_3O formation. However, as mentioned above, the path from **B** or **C** to **F** probably does not exist. Our results thus indicate that once HPD is made it cannot be photolyzed with photons of $\lambda > 400$ nm to produce C_3O or propynal.

The outlet from the $C_3{\cdot}H_2O$ complex through TS2 involves a single-step rotation of the H_2O with H loss. (It should be kept in mind that the process initially begins with excitation of C_3 and that the barrier TS2 is a minimum energy.) The product, **G**, is the hub of several paths leading to formation of **B**, **C**, **D**, $C_3O + H_2$, and $C_3O + 2H$. The formation processes leading to **B**, **C**, and **D** by H atom capture are calculated to be very exothermic. The barrier to the process **G** → **B** is calculated as 27.3 kcal/mol. While this is well within the photon energy limit, the actual barrier is ca.15 kcal/mol smaller due to a singlet−triplet surface crossing (Figure 5). C_3O is formed by both hydrogen abstraction in TS6 and dissociation in TS4. All paths leading out of **G** lie well within the experimental energy limit and should be rapid reactions under the experimental photolysis conditions.

In summary, the two most favorable routes to tricarbon oxide found in this work are **A** → TS2 → **G** → TS4 → $C_3O + 2H$ and **A** → TS2 → **G** → TS6 → $C_3O + H_2$ (these routes are marked by solid lines in Figure 4). The most favorable pathway to propynal is **A** → TS2 → **G** → **D** → **E**. With a excitation wavelength ≥ 400 nm, it is not possible to form either propynal or C_3O from **B** or **C**, the HPD rotamers. However, as shown in a previous study,[2] with an excitation wavelength of $280 \leq \lambda \leq 320$ nm, propynal may be formed from the HPD isomers.

B. Bimolecular Reactions Forming C_3O. After deposition many carbon species are present in the matrix. Carbon atoms and C_2 exist in relatively high abundance and, to a lesser extent, so do C_3 and the $C_3{\cdot}H_2O$ complex. In the previous section it was shown how the $C_3{\cdot}H_2O$ complex could, by sequential loss of hydrogen atoms, form C_3O. The large abundance of C atoms and C_2 means that the probability of bimolecular reactions occurring in the matrix may be high if the reactions involving them are energetically favorable. In this section we examine whether these reactions are indeed possible.

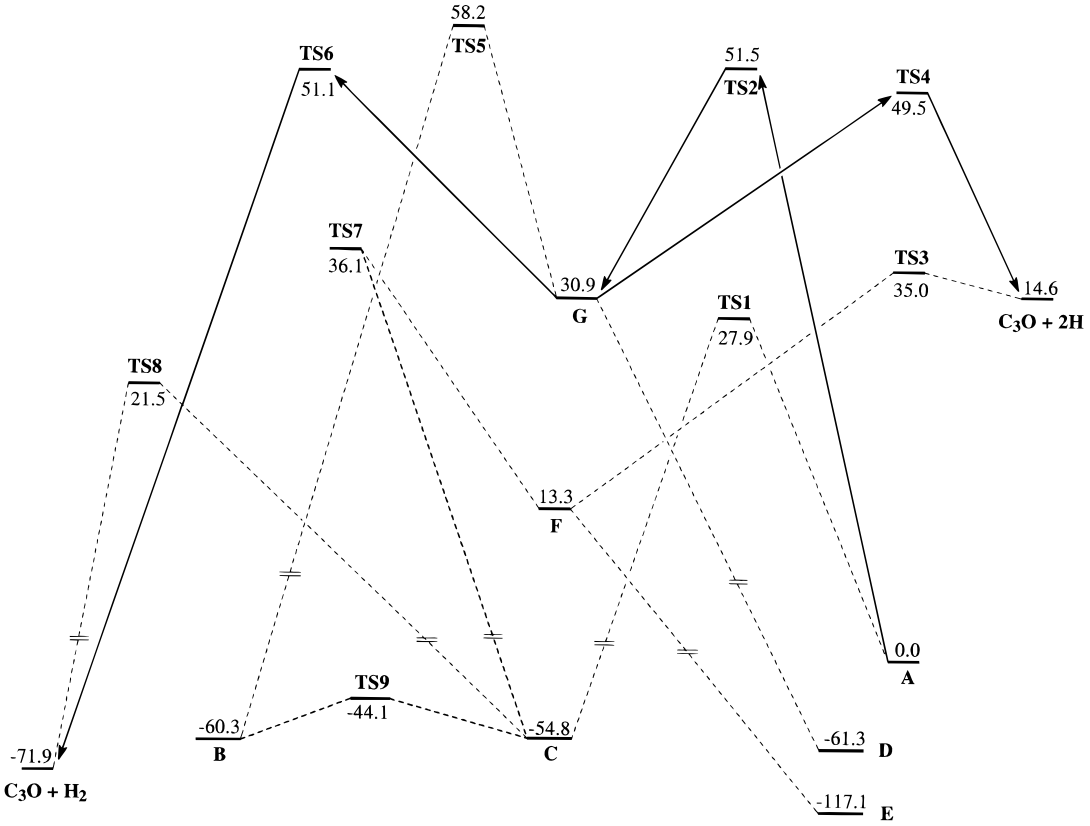

Figure 4. Potential surface for all C_3H_2O species considered in the present work. Values are zero-point-corrected energies relative to the $C_3{\cdot}H_2O$ complex (in kcal/mol). Favored routes to C_3O from the $C_3{\cdot}H_2O$ complex (**A**) are drawn with solid lines.

We have attempted to model the ground and excited state potential surface of the reaction

$$C_2 + CO + h\nu \rightarrow C_3O \qquad (2)$$

Both C_2 and CO have singlet ground states; however, despite the fact that this reaction is predicted to be exothermic by 85.5 kcal/mol (zero-point corrected), an extensive search of the singlet surface yielded no transition state that would form C_3O. The only transition state located was a T-shaped structure for the migration of CO around C_2 (i.e. $OCC_1C_2 \leftarrow TS \rightarrow C_1C_2$-CO). A transition state (TS10; cf. Figure 3) connecting ($^3\Pi$) C_2 and ($^1\Sigma^+$) CO to C_3O was found on the triplet surface. The $^3\Pi$ state of C_2 was used since the singlet−triplet separation in C_2 is known to be just 716 cm^{-1} (2.0 kcal/mol; our calculations find a separation of 5.0 kcal/mol), with many other allowed triplet transitions falling within the photolysis range of these experiments, including the well-known Swan system at ∼19 400 cm^{-1}.[11] At the MP2 level TS10 is predicted to lie just 0.2 kcal/mol above the ($^3\Pi$) C_2 and ($^1\Sigma^+$) CO reactants, but 19.0 kcal/mol above C_3O. Recently, Woon and Herbst[12] found this transition state at the MCSCF/cc-pVTZ level to be 32.9 kcal/mol above C_3O and 12.7 kcal/mol above C_2 and CO. The height of this barrier is obviously very dependent on the multiconfigurational nature of this calculation. This is almost certainly due to the well-known nondynamical correlation effects in C_2, resolved only in very comprehensive calculations.[13]

Another potentially important process is

$$C_2 + H_2O \rightarrow C_2{\cdot}H_2O \qquad (3a)$$

$$C_2{\cdot}H_2O + h\nu \rightarrow C_2O + 2H \text{ or } H_2 \qquad (3b)$$

This is a two-step sequence where the $C_2{\cdot}H_2O$ complex is first formed (3a) and then followed by photolysis to C_2O and 2H or H_2 (3b). The latter reaction assumes that a process similar to the C_3O formation mechanism exists for the production of C_2O. The presence of C_2O may have important consequences, which are elaborated below. Like the $C_3{\cdot}H_2O$ complex, the $C_2{\cdot}H_2O$ complex is expected to be weakly bound, more than likely forming only in the condensed phase. However, our theoretical results do not show any stable minimum for the $C_2{\cdot}H_2O$ complex. This is in contrast to the results on the $C_n{\cdot}H_2O$ series, in which stable complexes were found for $n = 3-9$.[14]

The presence of CO in the matrix is important because a number of reactions provide simple exothermic paths to C_3O formation.

$$C + CO + h\nu \rightarrow C_2O \qquad (4a)$$

$$C + C_2O + h\nu \rightarrow C_3O \qquad (4b)$$

DeKock and Weltner[15] have shown experimentally that the sequential reaction of carbon atoms with CO and C_2O can produce C_3O in an Ar matrix at 4 K. Our results indicate that the reactions of ^3P carbon atom with CO and C_2O will be exothermic by 63.7 and 178.7 kcal/mol, respectively. Results from density functional calculations show that, with the exception of CO, the reactions of (^3P) C atoms with C_nO species are all exothermic by at least 130 kcal/mol.[14] We have found experimentally that upon annealing in an Ar matrix, the C_3O increases while the realtively small concentration of CO present shows no decline. This observation supports the $C + C_2O \rightarrow C_3O$ aggregation reaction, but not the $C_2 + CO \rightarrow C_3O$ reaction.

The following reaction is a two-step process in which two C_2O molecules combine to form butatrienedione (C_4O_2), fol-

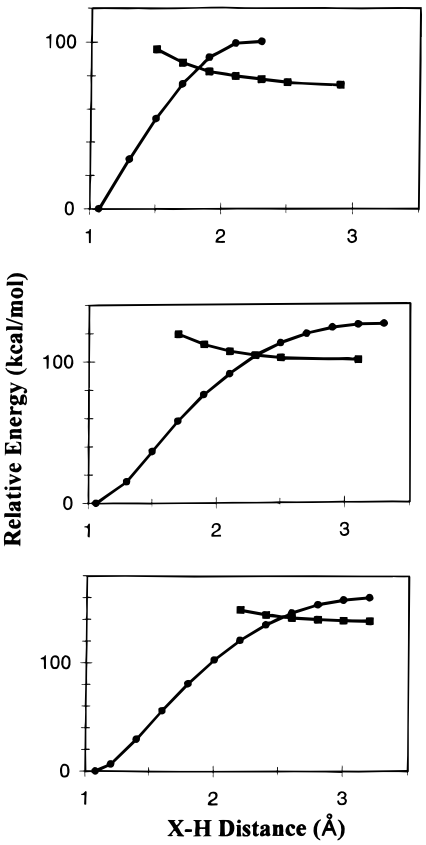

Figure 5. Top: Relative energies of the singlet (circles) and triplet (squares) surfaces of cis-HPD (**C**) as a function of OH bond length. Note that the triplet surface approaches the sum of the H atom and the **F** species at infinite separation (68.1 kcal/mol). Energies are relative to the fully optimized energy of cis-HPD. Middle: Relative energies of the singlet (circles) and triplet (squares) of trans-HPD (**B**) as a function of CH bond length. Note that the triplet surface approaches the sum of the H atom and the **G** species at infinite separation (98.0 kcal/mol). Energies are relative to the fully optimized energy of trans-HPD. Bottom: Relative energies of the singlet (circles) and triplet (squares) surfaces for H atom dissociation from propynal (**E**) as a function of OH bond length. Note that the triplet surface approaches the sum of the H atom and the **F** species at infinite separation (130.4 kcal/mol). Energies are relative to the fully optimized energy of propynal (**E**).

lowed by photolysis to C_3O and CO:

$$2C_2O + h\nu \rightarrow C_4O_2 \quad (5a)$$

$$C_4O_2 + h\nu \rightarrow C_3O + CO \quad (5b)$$

The former reaction is calculated to be 137.4 kcal/mol exothermic, while the latter is predicted to be endothermic by ca. 12 kcal/mol. The endothermicity of 5b is not a problem since it is known that C_4O_2 photodissociates into C_3O and CO with $\lambda > 400$ nm.[16] Results of a two-configuration-MCSCF calculation[16] indicate that an avoided crossing occurs when the $^1B_u \leftarrow {}^1A_g$ electronic transition of C_4O_2 at 412 nm is correlated with the C_3O and CO products. The barrier created by this crossing has a maximum energy less than 70 kcal/mol and will be an available path in the experiments discussed here.

While the addition of carbon atoms and molecules to oxygen-containing species has been considered, another reaction, the addition of oxygen atoms to carbon species, is possible as well. In the condensed phase, water molecules may serve as a source of oxygen atoms. Woon and Herbst[12] have recently shown that the process of making C_3O by adding an oxygen atom to C_3 proceeds over a very small barrier (1.8 kcal/mol) but is rather exothermic (99.6 kcal/mol) overall. While this small barrier is sufficient to prevent reaction in the gas phase, a photochemically driven process in the condensed phase may be possible. While these types of reactions were not investigated theoretically here, they may be an important pathway to formation of C_nO molecules.

IV. Conclusions

The following conclusions on the photolysis of the $C_3 \cdot H_2O$ complex with $\lambda \geq 400$ nm have been reached in the present work. (1) The $C_3 \cdot H_2O$ complex is a precursor to C_3O and propynal formation. (2) Photolysis of the complex leads to the HPD isomers **B** and **C** through the transition state TS1. C_3O and propynal could be formed from the HPD isomers via molecule **F**; however, the barrier heights leading from the HPD isomers prevent the direct formation of either molecule. (3) Photolysis of the $C_3 \cdot H_2O$ complex through TS2 yields molecule **G**. This molecule produces molecules **B** or **D** through H atom capture, or C_3O and H atom via hydrogen atom dissociation over TS4 or via abstraction through TS6. (4) The simultaneous formation of propynal and C_3O during $\lambda \geq 400$ nm photolysis in this scheme is entirely different from the mechanism in which HPD is an intermediate to the production of propynal. While the previous mechanism[3] involved H atom migration along the molecular backbone, the present mechanism relies on H atom dissociation and recombination (and, by inference, diffusion) in the condensed medium. (5) There is some experimental evidence that bimolecular reactions such as involving C atoms and simple C_nO species may be instrumental in forming C_3O.

In this and our previous paper, attention has been focused on the mechanisms of complex organic molecule formation via the $C_3 \cdot H_2O$ complex in the condensed phase. It has been pointed out that such reactions could occur in the mantles of interstellar dust grains. Both propynal and tricarbon oxide are known to exist in the interstellar medium in approximately equal abundances. The hypothesis of molecular formation in grain mantles is not new. In 1968 Williams[17] suggested that H atoms diffusing through grain mantles could react with trapped molecules and atoms to form hydrogenated products. Later, the diffusion of H atoms was proposed for the formation of NH_3, H_2O, H_2CO, and CH_3OH, among others.[18] Owing to the low temperature of dark clouds, most species in interstellar space would be expected to condense onto cold grain surfaces. These molecules would be part of a "soup" of reactive molecules containing H, C, N, and O atoms. Grain mantles such as these, exposed to unfiltered radiation, could be important factories for the production of more complex molecules such as the ones examined here.

Acknowledgment. The authors wish to acknowledge the National Aeronautics and Space Administration for its support of this research.

References and Notes

(1) Ortman, B. J.; Hauge, R. H.; Margrave, J. L.; Kafafi, Z. H. *J. Phys. Chem.* **1990**, *94*, 7973.

(2) Szczepanski, J.; Ekern, S. P.; Vala, M. *J. Phys. Chem.* **1995**, *99*, 8002.

(3) Ekern, S. P.; Szczepanski, J.; Vala, M. *J. Phys. Chem.* **1996**, *100*, 16109.

(4) Frisch, M. J.; Trucks, G. W.; Schlegel, H. B.; Gill, P. M. W.; Johnson, B. G.; Robb, M. A.; Cheeseman, J. R.; Keith, T.; Petersson, G. A.; Montgomery, J. A.; Raghavachari, K.; Al-Laham, M. A.; Zakrzewski, V. G.; Ortiz, J. V.; Foresman, J. B.; Peng, C. Y.; Ayala, P. Y.; Chen, W.; Wong, M. W.; Andres, J. L.; Replogle, E. S.; Gomperts, R.; Martin, R. L.; Fox, D. J.; Binkley, J. S.; Defrees, D. J.; Baker, J.; Stewart, J. P.; Head-Gordon, M.; Gonzalez, C.; Pople, J. A. *GAUSSIAN 94*, Revision B.2; Gaussian, Inc.: Pittsburgh, PA, 1995.

(5) Farnell, L.; Radom, L. *Chem. Phys. Lett*. **1982**, *91*, 373.
(6) Judeikis, H. S.; Flournoy, J. M.; Siegel, S. *J. Chem. Phys*. **1962**, *37*, 2272.
(7) Muto, H.; Toriymama, K.; Nunome, K.; Iwasaki, M. *Radiat. Phys. Chem*. **1982**, *19*, 201.
(8) Hiraoka, K.; Yamashita, A.; Yachi, Y.; Aruga, K.; Sato, T.; Muto, H. *Astrophys. J.* **1995**, *443*, 363.
(9) Hiralka, K.; Ohashi, N.; Kihara, Y.; Yamamoto, K.; Sato, T.; Yamashita, A. *Chem. Phys. Lett.* **1994**, *229*, 408.
(10) Takahashi, J.; Yamashita, K. *J. Chem. Phys*. **1996**, *104*, 6613.
(11) Weltner, W., Jr.; Van Zee, R. *Chem. Rev.* **1986**, *89*, 1713.
(12) Woon, D. E.; Herbst, E. *Astrophys. J*. **1996**, *465*, 795.
(13) Bauschlicher, C. W., Jr.; Langhoff, S. R. J. *J. Chem. Phys*. **1987**, *87*, 2919.
(14) Ekern, S. P.; Szczepanski, J.; Vala, M. Unpublished results.
(15) DeKock, R. L.; Weltner, W., Jr. *J. Am. Chem. Soc*. **1971**, *93*, 7106.
(16) Maier, G.; Reisenauer, H. P.; Balli, H.; Brandt, W.; Janoschek, R. *Angew. Chem., Int. Ed. Engl*. **1990**, *29*, 905. The authors report photodissociation of C_4O_2 with $\lambda = 436 \pm 10$ nm.
(17) Williams, D. A. *Astrophys. J*. **1968**, *151*, 935.
(18) (a) Tielens, A. G. G. M.; Hagen, W. *Astron. Astrophys*. **1982**, *114*, 245. (b) Tielens, A. G. G. M.; Allamandola, L. J. In *Interstellar Processes*: Hollenbach, D. J., Thronson, H. A., Jr., Eds.; D. Reidel: Dordrecht, 1987; p 397.